

**Question n. 1**

Consider the drive oscillator of a MEMS gyroscope. Explain in motivated details (i) which option is preferred between comb-finger and parallel-plate capacitors, for actuation and detection of the drive resonator.

Discuss then in details (ii) about the advantages and drawbacks of choosing between a trans-resistance or trans-capacitance front-end circuit (in the discussion, refer to typical values of passive components).

Finally, assume that your implemented drive resonator shows a different behaviour with respect to theoretical predictions, and you suspect that electrostatic fringe effects of capacitors may be responsible. Describe (iii) a possible simulation approach to investigate this problem.

The scale-factor of a MEMS gyroscope is proportional to the drive displacement  $x_d$ . Therefore, in order to maximize the transduction, it is appropriate to have a drive motion as large as possible. Even if parallel plates are known to apply a large transduction per unit area for small displacements, it is also known that their linearity is very poor (few % error) once motion is larger than 10% of the gap or so. As target displacements in gyroscopes are in the order of 5 to 10  $\mu\text{m}$ , using parallel plates would be very inconvenient. Additionally, for an oscillator it is good to have a large-quality-factor resonant element: when using parallel plates, squeezed-film damping decreases the Q and thus the purity of the oscillation. A low Q is detrimental also for feedthrough effects and noise.

Using comb fingers, instead, the issues above are bypassed: large motion amplitude could be obtained with no transduction nonlinearity, neither for drive actuation, nor for drive detection:

$$\eta = \frac{F_{act}}{v_a} = \frac{i_m}{\dot{x}} = \frac{2\epsilon_0 h N_{CF}}{g} V_{rot} = \frac{2C_0}{L_{ov}} V_{rot}$$

Even if the transduction force per unit applied voltage is lower than for parallel plates, the absence of squeezed-film damping avoids reduction of the quality factor, thus enabling large displacements at resonance due to the large amplification obtained through the Q factor.

It is then possible to pass from the motional current into a voltage through either a charge amplifier or a trans-resistance amplifier. The latter would be potentially an interesting solution, as it applies no quadrature phase shift, and would thus require no 90-deg shifting stage in the drive loop. However, there are two reasons why a trans-resistance amplifier is not preferred:

- (1) its output signal is proportional to drive velocity, rather than drive displacement. As in a gyroscope we need an AGC controlling the drive displacement, it is wise to have a signal within the drive loop which is proportional to this quantity. Using a charge amplifier, its output will be proportional to the drive displacement and could be used directly to feed the AGC.
- (2) to minimize noise from the feedback resistance, a high  $R_F$  value is preferred. However, to operate with a trans-resistance amplifier, the pole is required to be at a frequency much larger than resonance, which is in huge trade-off with having a large resistance (which pushes the pole downward). In turn, there is no practical possibility to use large resistors (e.g. several M $\Omega$ ) combined with available integrated capacitances (at least 50-100 fF) and correctly place the poles. Using a charge amplifier, instead, though topologically identical, we have a chance to set the gain through a capacitance (e.g. in the 100 fF to 1 pF range), while keeping the pole at low frequency (well before resonance) through an extremely large resistance. This can be even implemented with off-mode transistors because, even if their value is not repeatable, the key point here is that it is very large, causing very low noise.

Often experimental results are not in line with theory, because of unavoidable approximations we use in developing calculations. This is where simulators become helpful. A typical case is when we need to simulate capacitors, for which we always neglect fringe effects during theoretical developments.

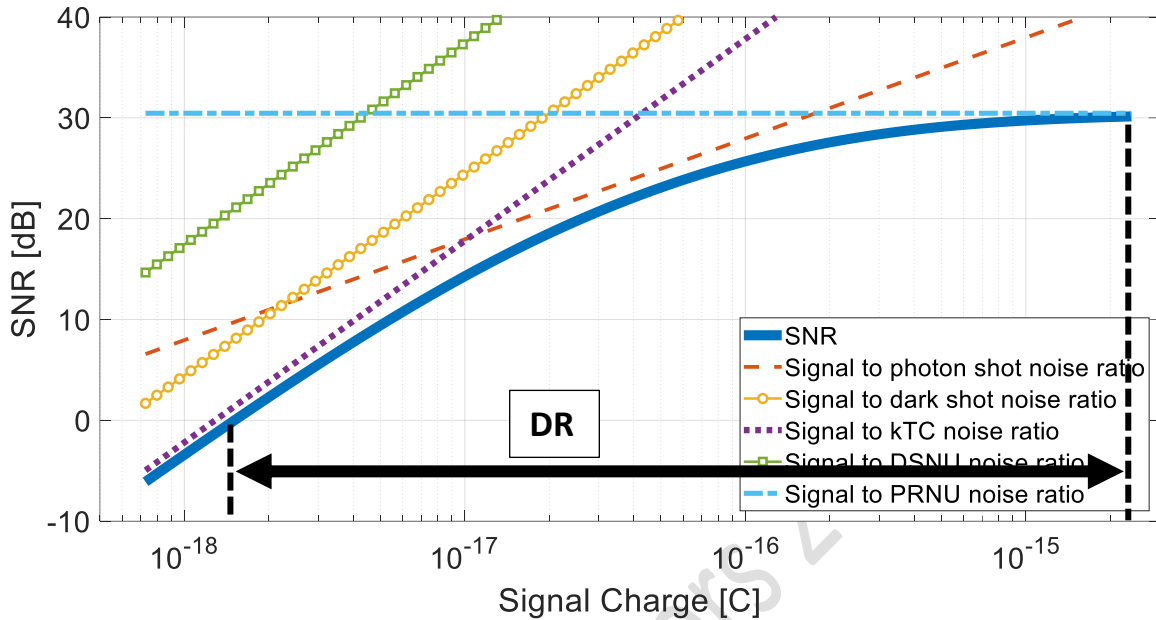
A simulation could be therefore setup to verify the discrepancy: the flow would require to first create the geometry of the capacitor (2D or, even better, full 3D model), surrounded by air. Then we would need to set our boundary conditions, forcing e.g. a constant potential on the two surfaces of the capacitor. A grid of points (the finite elements) is then created. The simulator will finally solve the differential equations associated to the electrostatic domain (the Poisson equation, in essence), providing the solution in terms of electric field distribution in all these finite elements. The value of the capacitance can be thus evaluated through the simulator.

Repeating the simulation for different displacements, one can calculate the transduction factor  $dC/dx$  and cross check the simulated value against theory.

**Question n. 2**

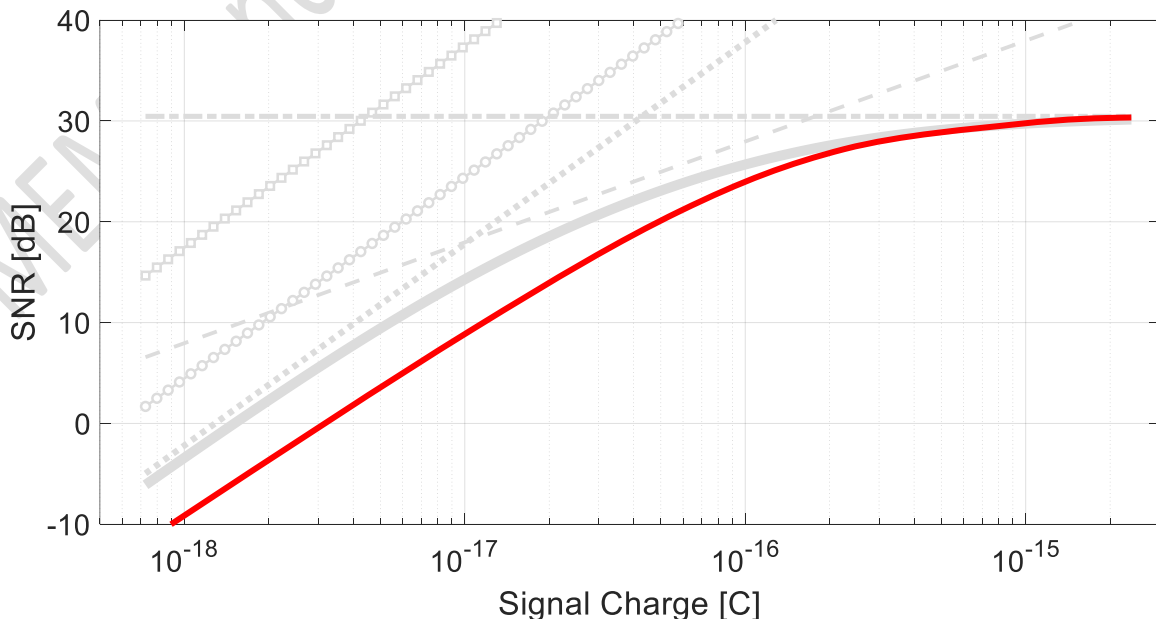
A 3T imaging sensor is characterized by the parameters listed in the Table. Given the graph below, showing the various measured SNR contributions vs the signal charge:

Integration time	$t_{int}$	10	ms
MOS channel width	$W_{MOS}$	150	nm
MOS channel length	$L_{MOS}$	90	nm
Gate oxide thickness	$t_{ox}$	5	nm



- (i) calculate, the dark current, the %PRNU, the %DSNU and the depletion capacitance (suggestion: for the sake of simplicity, when possible, do your calculations for the points where  $SNR = 20 \text{ dB} = 10$ );
- (ii) evaluate the dynamic range, clearly indicating the procedure and showing the relevant points also on the graph above;
- (iii) calculate the difference between the theoretical maximum SNR and the measured maximum SNR;
- (iv) write the complete expression of the SNR, explicitly in terms of charge: then, using the second provided figure below, redraw the SNR graph (the total only) vs signal charge in case the integration time is increased to 100 ms (note: previous values are shown in grey to facilitate the new graphical solution).

**Physical Constants**  
 $\epsilon_{Si} = 8.85 \cdot 10^{-12} \text{ F/m} \cdot 11.7$ ;  
 $\epsilon_{ox} = 8.85 \cdot 10^{-12} \text{ F/m} \cdot 4.1$ ;  
 $k_b = 1.38 \cdot 10^{-23} \text{ J/K}$ ;  
 $q = 1.6 \cdot 10^{-19} \text{ C}$ ;  
 $T = 300 \text{ K}$ .



(i)

The first point can be addressed by writing different expressions of the SNR referred, each time, to a different noise source, and comparing them to the points we find on the graph. As suggested, where possible we refer to 20 dB which means 10 in linear scale.

Starting from dark current shot noise:

$$SNR_{dark} = 20 \cdot \log_{10} \frac{Q_{ph}}{\sqrt{q i_d t_{int}}} = 20 \text{ dB} \rightarrow \frac{Q_{ph}}{\sqrt{q i_d t_{int}}} = 10$$
$$\rightarrow i_d = \frac{(6 \cdot 10^{-18} \text{ C})^2}{100 \cdot 1.6 \cdot 10^{-19} \cdot 10 \text{ ms}} = 0.22 \text{ fA}$$

We then analyse DSNU:

$$SNR_{DSNU} = 20 \cdot \log_{10} \frac{Q_{ph}}{i_d t_{int} \sigma_{DSNU}} = 20 \text{ dB} \rightarrow \frac{Q_{ph}}{i_d t_{int} \sigma_{DSNU}} = 10$$
$$\rightarrow \sigma_{DSNU} = \frac{1.4 \cdot 10^{-18} \text{ C}}{10 \cdot 0.22 \text{ fA} \cdot 10 \text{ ms}} = 0.06 \rightarrow \sigma_{DSNU\%} = 6\%$$

Next, we pass to kTC noise to evaluate the depletion capacitance:

$$SNR_{kTC} = 20 \cdot \log_{10} \frac{Q_{ph}}{\sqrt{k_B T C_{int}}} = 20 \text{ dB} \rightarrow \frac{Q_{ph}}{\sqrt{k_B T C_{int}}} = 10$$
$$\rightarrow C_{int} = \frac{(1.3 \cdot 10^{-17} \text{ C})^2}{1.38 \cdot 10^{-23} \text{ J/K} \cdot 300 \text{ K} \cdot 100} = 0.4 \text{ fF}$$

The average depletion capacitance is calculated by subtracting to this value the MOS capacitance:

$$C_{dep} = C_{int} - C_{MOS} = C_{int} - \frac{\epsilon_{OX} A_{MOS}}{t_{MOS}} = 0.4 \text{ fF} - 0.1 \text{ fF} = 0.3 \text{ fF}$$

Finally, we consider PRNU, where there is no point at 20 dB and we thus consider the value at 30 dB, which is indeed independent of the signal:

$$SNR_{PRNU} = 20 \cdot \log_{10} \frac{Q_{ph}}{i_{ph} t_{int} \sigma_{PRNU}} = 30 \text{ dB} \rightarrow \frac{Q_{ph}}{Q_{ph} \sigma_{PRNU}} = 31.6$$
$$\rightarrow \sigma_{PRNU} = \frac{1}{31.6} = 0.03 \rightarrow \sigma_{PRNU\%} = 3\%$$

(ii)

The DR is easily evaluated looking for two points on the graph: the saturation value on the x-axis, which is roughly  $2.1 \cdot 10^{-15} C$ , and the point where SNR equals 0 dB, reading the corresponding coordinate on the x-axis, which is  $1.4 \cdot 10^{-18} C$ . The DR is thus:

$$DR = 20 \cdot \log_{10} \frac{2.1 \cdot 10^{-15}}{1.4 \cdot 10^{-18}} = 63 \text{ dB}$$

(iii)

The theoretical maximum SNR is due to photon shot noise and does not foresee the presence of PRNU. In that case, the maximum SNR would be that of a typical Poisson process, given by the maximum number of electrons we can collect in the photodiode:

$$\begin{aligned} SNR_{max} &= 20 \cdot \log_{10} \sqrt{N_{el}} = 20 \cdot \log_{10} \sqrt{\frac{Q_{ph_{max}}}{q}} = 20 \cdot \log_{10} \sqrt{\frac{2.1 fC}{1.6 \cdot 10^{-4} fC}} = \\ &= 20 \cdot \log_{10} \sqrt{13125} = 41.2 \text{ dB} \end{aligned}$$

The difference of about 11 dB with respect to the value observed on the graph is indeed due to PRNU.

(iv)

The SNR, explicitly written in terms of photocharge (which is the quantity on the x-axis in our graph), is:

$$20 \cdot \log_{10} \frac{Q_{ph}}{\sqrt{Q_{ph} \cdot q + i_d t_{int} \cdot q + k_B T C_{int} + (Q_{ph} \sigma_{PRNU})^2 + (i_d t_{int} \sigma_{DSNU})^2}}$$

Therefore, we can observe that:

- at low photo-charge values, where kTC, dark shot and DSNU dominate, the expression is dependent on the integration time, and we can expect a worsening when increasing  $t_{int}$ .

$$20 \cdot \log_{10} \frac{Q_{ph}}{\sqrt{i_d t_{int} \cdot q + k_B T C_{int} + (i_d t_{int} \sigma_{DSNU})^2}}$$

- at intermediate photocharge values, shot noise dominates. The expression becomes:

$$20 \cdot \log_{10} \frac{Q_{ph}}{\sqrt{Q_{ph} \cdot q}}$$

And it thus independent of the integration time.

- finally, at large photocharge values, PRNU dominates but the expression still remains independent of the integration time:

$$20 \cdot \log_{10} \frac{Q_{ph}}{Q_{ph} \sigma_{PRNU}} = 20 \cdot \log_{10} \frac{1}{\sigma_{PRNU}}$$

We conclude that for 100 ms integration time the graph changes only where signal independent noise dominates. We can calculate the new SNR e.g. for a low-value x-axis coordinate in the graph:

$$20 \log_{10} \frac{10^{-18} C}{\sqrt{0.22 fA \cdot 100ms \cdot q + k_B T 0.4 fF + (0.22 fA \cdot 100ms 0.06)^2}} = -8.4 dB$$

The corresponding new graph is thus shown in the figure: the slope will be +20 dB/dec until we reach the region where photon shot and PRNU dominate.

MEMS and Microsensors 2012/2014

**Question n. 3**

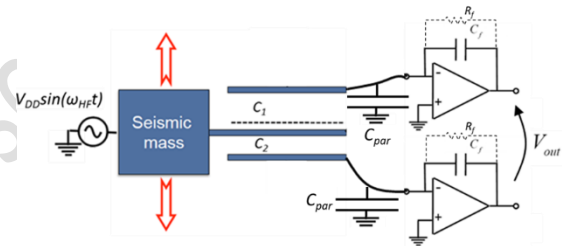
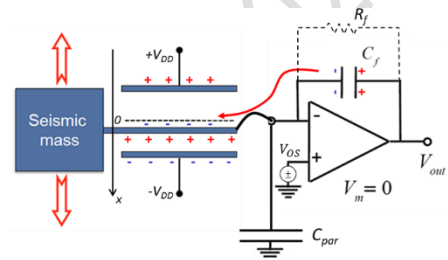
A MEMS accelerometer is operated with the two schemes shown in the figure and with the parameters given in the Table:

Mass	9 nkg
Native resonance	3.8 kHz
Single ended capacitance	225 fF
Parallel plate gap	1.4 μm
V <sub>DD</sub> voltage	2.2 V
Modulation high frequency	400 kHz
FSR	±32 g
Amplifier supply voltage	±3 V
Quality factor	2.5
Total measured noise	18 μg/√Hz
Parasitic capacitance	8 pF
Amplifier offset voltage	1 mV

- (i) calculate the target sensitivity  $V_{out}/a$  and evaluate the optimal feedback capacitance;
- (ii) the measured noise for the first configuration, in terms of acceleration density is 18 μg/√Hz. Evaluate the amplifier voltage noise density;
- (iii) complete the two chains drawing the missing stages to the digital output;
- (iv) which is the effect of an amplifier offset of 1 mV, in terms of input referred acceleration offset, for the two situations?

**Physical Constants**

$\epsilon_0 = 8.85 \cdot 10^{-12}$  F/m;  
 $k_b = 1.38 \cdot 10^{-23}$  J/K;  
 T = 300 K.



i)

Assuming the output swing of the amplifiers to be fully exploited, the target sensitivity  $V_{out}/a$  can be computed as:

$$\frac{V_{out}}{a} = \frac{V_B}{FSR} = \frac{\pm 3 \text{ V}}{\pm 32 \text{ g}} = 93.75 \text{ mV/g}$$

The charge amplifier feedback capacitance  $C_F$  can be computed inverting the expression for the sensitivity of a differential parallel-plate accelerometer:

$$SF = \frac{V_{out}}{a} = 2 \frac{V_{DD}}{C_F} \frac{C_0}{g} \cdot \frac{1}{\omega_0^2}$$

Note that the radial resonance frequency in operation  $\omega_0$  is affected by electrostatic softening, thus being lower than the native (mechanical) resonance  $\omega_n$ :

$$\omega_0 = \sqrt{\frac{k_m + k_{elec}}{m}} = \sqrt{\frac{m\omega_0^2 - V_{DD}^2 \frac{C_0}{g^2}}{m}} = 2\pi \cdot (3.36 \text{ kHz})$$

We can thus compute:

$$C_F = \frac{2V_{DD} \frac{C_0}{g} \cdot \frac{1}{\omega_0^2}}{SF} = 165.7 \text{ fF}$$

ii)

The overall input-referred noise power spectral density  $S_{a,TOT}$  is given by the sum of thermo-mechanical and electronic contributions:

$$S_{a,TOT} = NEAD^2 + S_{a,eln} = \frac{4k_B T \omega_0}{mQ} + \frac{S_{v,OA} \left(1 + \frac{C_p + 2C_0}{C_F}\right)^2}{SF^2} = (18 \mu\text{g}/\sqrt{\text{Hz}})^2$$

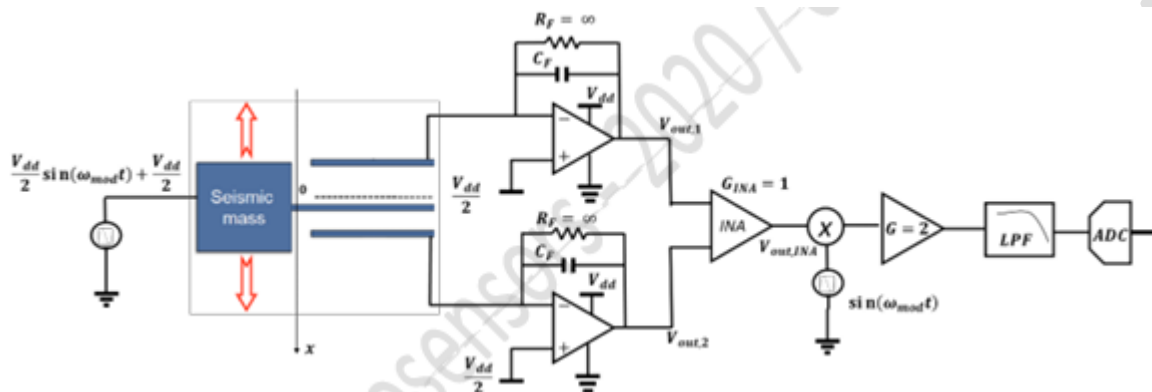
We neglect the resistance, as usually this can be made large enough not to affect the result. Since the NEAD can be computed from the data ( $12.7 \mu\text{g}/\sqrt{\text{Hz}}$ ), we can solve for the amplifier voltage noise power spectral density  $S_{v,OA}$ :

$$S_{v,OA} = \frac{(S_{a,TOT} - NEAD^2) \cdot SF^2}{\left(1 + \frac{C_p + 2C_0}{C_F}\right)^2} = (23 \text{ nV}/\sqrt{\text{Hz}})^2$$

iii)

For the first scheme, the output of the CA is directly connected to the ADC.

In the second scheme, the differential CA output is converted to single-ended by means of an INA, demodulated (multiplying by the AC rotor signal) and low-pass filtered to attenuate the second harmonic. The output of the LPF can be then fed to an ADC. The scheme is thus similar to the figure below.



iv)

For the first readout scheme, the offset voltage of the amplifier is directly transferred to the output, as in DC this stage behaves as a buffer; this results in an input-referred offset  $a_{os}$ :

$$a_{os} = \frac{V_{os}}{SF} = 10.7 \text{ mg}$$

In the second readout scheme, the signal is modulated at the rotor voltage modulation frequency  $\omega_{HF}$  and is thus unaffected by the baseband (DC) offset of the charge amplifier. After the demodulation, the signal is brought back to baseband, while the offset shifts at high frequency, resulting in no input offset contribution coming from the amplifiers.

MEMS and Microsensors 20/12/2024